

LAUR-92-1158

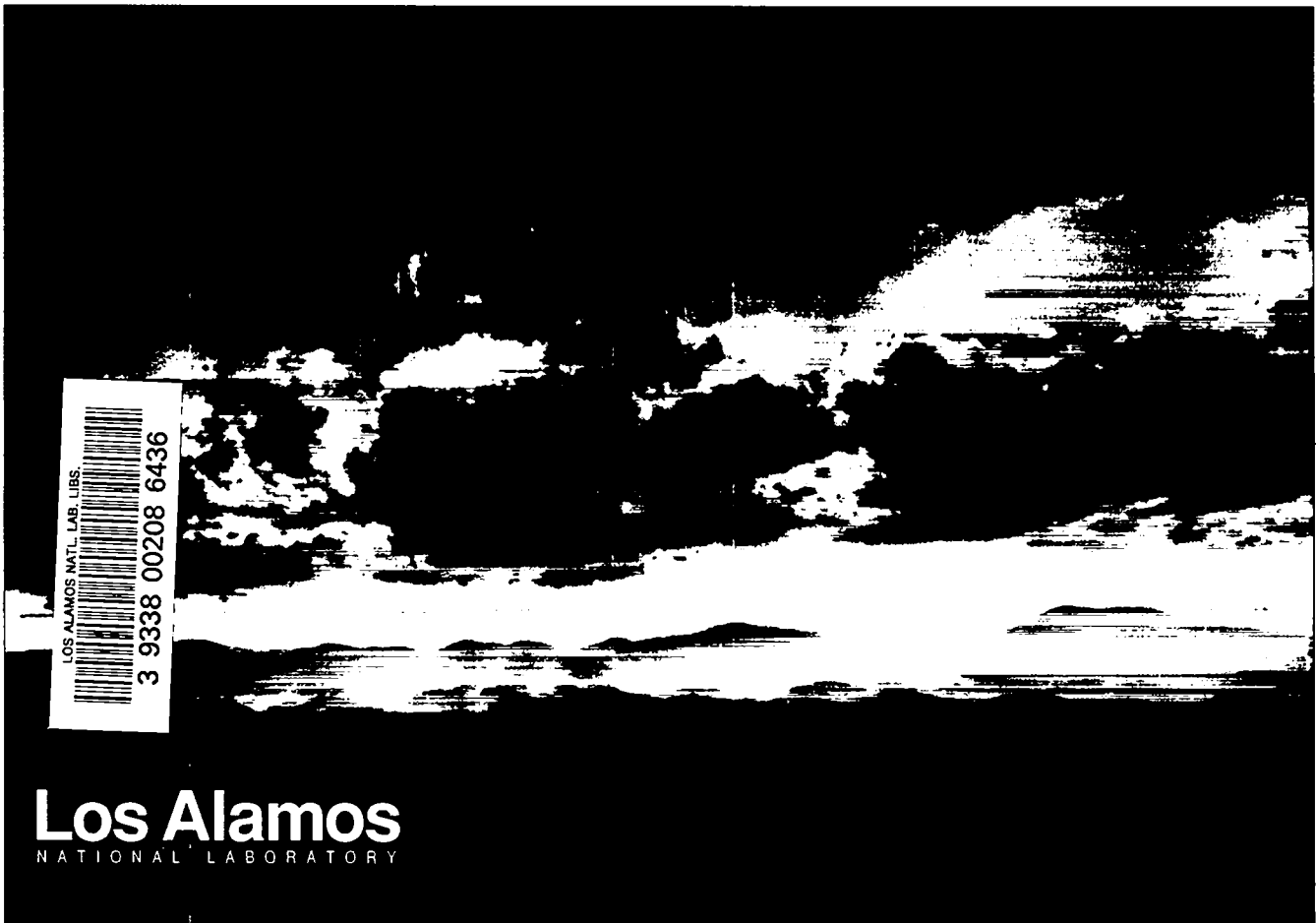
c.1

**DELINEATION OF SPALL ZONE FROM PRE/POST
SHOT REFLECTION STUDIES: PRELIMINARY
RESULTS FROM BEXAR**

**S. R. Taylor, A. H. Cogbill and T. A. Weaver
Los Alamos National Laboratory**

**R. Miller and D. Steeples
Kansas Geological Survey
The University of Kansas
Lawrence, Kansas 66046**

Los Alamos Source Region Project



LOS ALAMOS NATL. LAB. LIBS.
3 9338 00208 6436

Los Alamos
NATIONAL LABORATORY

Photograph by Chris J. Lundberg

DISCLAIMER

This report was prepared as an account of work sponsored by an agency of the United States Government. Neither the United States Government nor any agency thereof, nor any of their employees, makes any warranty, express or implied, or assumes any legal liability or responsibility for the accuracy, completeness, or usefulness of any information, apparatus, product, or process disclosed, or represents that its use would not infringe privately owned rights. Reference herein to any specific commercial product, process, or service by trade name, trademark, manufacturer, or otherwise, does not necessarily constitute or imply its endorsement, recommendation, or favoring by the United States Government or any agency thereof. The views and opinions of authors expressed herein do not necessarily state or reflect those of the United States Government or any agency thereof.

**DELINEATION OF SPALL ZONE FROM PRE/POST SHOT
REFLECTION STUDIES: PRELIMINARY RESULTS FROM BEXAR**

Steven R. Taylor
Allen H. Cogbill
Thomas A. Weaver

Group EES-3
Los Alamos National Laboratory
University of California
Los Alamos, NM 87545

Rick Miller
Don Steeples

Kansas Geological Survey
The University of Kansas
Lawrence, Kansas 66046

April 9, 1992



LAUR-92-1158

ABSTRACT

In order to delineate the lateral and depth extent of spall from a buried nuclear explosion, we have performed a high-resolution pre- and post-shot seismic reflection survey from BEXAR. Although the data quality were marginal due to poor wave propagation through the volcanic tuffs of Pahute Mesa, a number of interesting differences are observed on the pre- and post-shot surveys. On the pre-shot survey, a reflector (reflector "1") is observed at 250 ms (or about 150 m depth) using a stacking velocity of 1300 m/s. On the post-shot survey two reflectors are observed and a stacking velocity of 1150 m/s was used representing a 12% reduction in compressional velocity. With this stacking velocity, reflector "1" is recorded at 290 ms (still at about 150 m depth) and a new reflector "2" is observed at 210 ms (or about 100 m depth). These stacking velocities correspond well with available uphole travel times collected in U19ba and nearby U19ax (BEXAR and KEARSARGE emplacement holes, respectively).

The cause for the differences observed in the pre- and post-shot surveys may be due to one of two reasons. First, it is possible that the near-surface rocks were damaged as part of the spallation process (thus reducing the *in situ* velocities) and reflector "2" represents a spall detachment surface. However, analysis of acceleration data collected close to the reflection line suggests that the ground motions were probably inadequate to damage the tuffs. Also, although the ground-motion data suggest that the reflection line was located very close to the edge of spall, no evidence of actual spallation was actually observed. The second hypothesis is that the near-surface velocities of the tuffs were altered by the change in saturation state due to extensive rains occurring between the pre- and post-shot surveys. Although the dependence of seismic velocity on saturation state is controlled by a number of complex factors, it cannot be ruled out.

INTRODUCTION

A number of studies have addressed the possible effects of spall on regional and teleseismic waveforms. The complexities introduced by spall on radiated signals can have an impact on monitoring capabilities. For example, Taylor and Randall (1989) showed examples of how spall may affect the performance of spectral discriminants. Burdick *et al.*, (1984; 1989) attributed anomalously large pP delays commonly observed for explosions to effects of spall for both teleseismic P waves and Pn. In a complete moment tensor inversion of the explosion HARZER, Patton (1988) discussed the effects of spall on the Lg phase. Simulation studies of spall by Barker *et al.*, (1990) indicate that spall may have a greater impact on regional signals (particularly Lg) in high-velocity environments such as those found at test sites of the former Soviet Union. Given the remarkable stability of Lg as a yield estimator in the Soviet Union [Hansen *et al.*, (1990)], it is important to understand the effects of spall on regional signals.

Much can be learned about spallation from observation of close-in acceleration waveforms. These can provide information on characteristic times, escape velocities, lateral extent, and depth of spall (giving the spalled mass) if adequately instrumented (e.g. Stump, 1985). However, for nuclear explosions it is prohibitively expensive to adequately sample the spall region. Typically, acceleration records are acquired at just the free surface and possibly in the emplacement hole and it is not possible to obtain a three-dimensional view of the spall process.

As an attempt to obtain an improved image of the lateral and depth extent of spall, we have conducted a pilot study assessing the utility of collecting pre- and post-shot reflection data from the spall zone for the NTS explosion BEXAR (Miller and Steeples, 1992). It is hoped that by comparing records from pre- and post-shot reflection surveys, some change can be observed due to the effects of spall on the local geology. In this report, we first review spall observations and models. Then we discuss results from the pre- and post-shot reflection experiment for BEXAR and describe future efforts.

SPALL OBSERVATIONS AND MODELS

Spall is defined as the parting of near-surface layers above a buried explosion. It is thought to be caused by the tensile failure from the interaction of an up going compressional wave with a down going tensile wave reflected from the free surface. The spalled surface layers are sent into ballistic free fall and eventually impact with the earth. Free field and surface accelerometer records from spall have been described in a number of studies including Eisler *et al.*, (1966), Stump (1985), and Patton (1990) for both nuclear and chemical explosions. Spall is observed to initiate near the free surface and propagate downwards and radially away from the explosion. The spalled material detaches and begins to free fall (as evidenced by -1g accelerations). Rejoin begins first at depth and distance and propagates upward and towards the ground zero initiation point. The resultant acceleration records are generally similar to those in Figure 1 where the initial compressive wave is followed by the detachment, free fall, and subsequent rejoin (slapdown). Most previous studies of the effects of spall on far-field seismograms have concentrated on factors causing scatter in M_s versus yield relationships and $m_b - M_s$ discrimination (e.g. Sobel, 1978). For example, Rygg (1979) observed anomalous surface wave observations from certain eastern Kazakh explosions and attributed them to effects of spall closure (slapdown) which was studied theoretically by Viccelli (1973). The spall closure hypothesis of Viccelli predicts that spall can have significant effects on long-period surface waves.

Day *et al.*, (1983) have noted that the Viccelli (1973) spall closure model fails to conserve momentum and gives incorrect results. An equivalent elastic source model for spall involving vertical point forces has been developed by Day *et al.*, (1983) and Day and McLaughlin (1991) that conserves momentum. This model suggests that the main effect of spall will occur at higher frequencies than predicted by the Viccelli model, and that spall only has an effect on short period surface waves. This was confirmed by Patton (1988) in an attempt to obtain the explosion moment for the NTS explosion HARZER from a complete moment tensor inversion of fundamental- and higher-mode surface waves. It was found that spall can have a significant effect on the higher mode surface wave spectra and must be accounted for.

Effects of spall on teleseismic body waves have been studied by Bakun and Johnson (1973) who used a deconvolution procedure to separate spall and pP from the direct P wave for MILROW and CANNIKIN. Burdick *et al.*, (1984) attributed

anomalously large pP delays commonly observed for explosions to effects of spall. In their model, the signal from the spall detachment destructively interferes with the pP. The next signal that is radiated to the far field is actually generated by the spall slapdown which is incorrectly identified as pP. Springer (1974) attempted to measure delay times at teleseismic distances between the direct P wave and the slapdown arrival. Significant disagreement was observed between predicted delay times based on surface ground-zero accelerograms and measured delayed times.

Taylor and Randall (1989) investigated the effects of spall on explosion spectra. It was suggested that a spectral peak observed for a normally contained explosion was due to the superposition of a spall source on the explosion. The spectral peak appeared to be absent for a nearby overburied explosion with a small spall contribution. By comparing spectra from overburied explosions (having a small spall secondary source) with normally-buried explosions, Patton and Taylor (1990) attempted to separate out effects of spall from other secondary sources in explosion-generated Lg waves. It was found that it is difficult to isolate the effects of spall from other sources for NTS explosion spectra.

Using regional surface waves, Patton (1991) computed complete moment-tensor inversions for a suite of Pahute Mesa explosions to obtain the explosion moment (which should be a fundamental measure of the explosion yield). To constrain the inversion, it was required to use higher-mode surface waves (low-frequency Lg) which are sensitive to the effects of spall. It was therefore necessary to derive spall scaling relationships from available close-in acceleration data for Pahute Mesa (Patton 1990). With this information, Patton (1991) was able to substantially reduce uncertainties in M_0 - yield relationships.

As discussed by Day *et al.*, (1983) and Stump (1985), the important parameters in modeling the effects of spall on far-field seismic waves are basically the spalled mass, escape velocities and characteristic times. The product of the spalled mass and velocity (momentum) controls the strength of the spall signature relative to the explosion. The characteristic times [pulse width and dwell time (i.e. the time of ballistic free flight separating the spall initiation from the slapdown)] control the frequency content of the radiated spall signals. For an impulsive response, the equivalent elastic surface load for an idealized spall model is given by

$$f_s(t) = v_0 m_s \delta(t) - m_s g [H(t) - H(t - T_s)] + v_0 m_s \delta(t - T_s) \quad (1)$$

where $\delta(t)$ is the delta function, $H(t)$ is the step function, g is the gravitational acceleration (9.8 m/s^2), m_s is the average spalled mass, and T_s is the dwell time. The dwell time is related to the escape velocity (v_0) through simple ballistics, $T_s = 2v_0/g$. The three terms in equation (1) correspond to the detachment, earth rebound during ballistic free flight of the spalled layer, and subsequent slapdown, respectively.

Using the spall model of Stump (1985) we can illustrate the effects of different parameters on radiated spectra. Figure 2 shows the effects of rise time and dwell time on source spectra. The spall signatures generate a peaked spectra whose maximum value is inversely proportional to the dwell time (i.e. spall signals having high escape velocities and hence long dwell times). The pulse width controls the high frequency decay of the spall spectrum. Physically, the pulse width can be affected by non-linear processes occurring in the near-source region (cf. App and Brunish, 1991; 1992) or can be used to simulate spall finiteness.

The importance of spall on regional seismic signals is further illustrated in Figure 3. The top portion of Figure 3 shows the results of the convolution of an explosion reduced velocity potential (RVP; left) with the vertical seismic response for a pure explosion point source calculated at 300 km (middle) to produce the complete response for an explosion (right). The explosion RVP was computed using a Mueller and Murphy (1971) model for a 100 KT explosion in tuff at 500 m depth. The Green's functions were computed using the technique of Kennett (1983) for a Basin and Range structure and are shown as reduced travel times. The Pg wavetrain arrives at a reduced time of about 25 seconds, the Lg at about 60 seconds and the Rayleigh waves at about 80 seconds. The bottom portion of the figure shows the equivalent representation for spall. The left portion shows the derivative of the spall acceleration time function (spall jerk) for a dwell time of 1.7 seconds and rise time of 0.4 seconds. This is convolved with a vertical point force response computed at the free surface (middle bottom) to produce the spall response (right bottom). The differences between the two sources are apparent from the complete responses shown on the right. It can be seen that the spall is a much more efficient generator of Lg and higher-mode surface waves relative to the explosion. This can be seen by the much larger Lg/Pg ratio for the spall response. Thus, depending on the scaling relationships, spall is expected to have a relatively small effect on P waves and a larger effect on Lg for a buried explosion. Also, because of its peaked spectrum (illustrated in Figure 2), it is expected that spall will affect only a narrow band of frequencies. For typical nuclear explosions, the maximum effect

will be for frequencies between approximately 0.3 to 5 Hz (which is an important frequency band for seismological studies).

PRE/POST SHOT REFLECTION RESULTS FOR BEXAR

The NTS explosion BEXAR was conducted on Pahute Mesa in hole U19ba on April 4, 1991 at 19:00:00.0 UT (Figure 4). BEXAR was detonated at a depth of 630 m and had an NEIS magnitude of 5.6. Due to the proximity of BEXAR to previous detonations, the geology in the region is known very well (Warren 1991, unpublished manuscript). The explosion was detonated in rhyolite, 27 m above the standing water level. Tuffs and rhyolites of the Timber Mountain Group are located at shallower depths (Figure 5). The large circle in Figure 4 outlines the expected lateral extent of spall and locations of surface fractures produced by surface motion from the BEXAR experiment.

Geophysical borehole measurements from U19ba are shown in Figure 6. The geophysical and geological characteristics of U19ba are very similar to those in nearby emplacement holes. Porosities and gas-filled porosities in U19ba range from 10 to 50% and 5 to 28%, respectively, in the upper 100 m. The strongest velocity and density contrasts appear to occur between depths of about 60 to 90 m in the vicinity of the contact between the Ammonia Tanks and Rainier Mesa tuffs.

Also shown in Figure 4 are the locations of the two pre- and post-shot reflection lines 1 and 2. Unfortunately, the data from line 1 (located about 500 m from ground zero) were contaminated by 60 Hz noise from a nearby powerline in the pre-shot experiment. Line 2 was located approximately 1.8 km from ground zero near the edge of the maximum expected lateral extent of spall. Details of the experiment are given in Miller and Steeples (1992). Both P wave and S wave reflection data were recorded. However, for this experiment, the recording bandwidth for the S waves was not adequate to obtain reliable data.

The P-wave data were acquired using a silenced 0.50-caliber seismic rifle and short, 2-m arrays of 3 to 40-Hz, vertical-component geophones. The data were recorded on an EG&G Geometrics 2401 seismograph, a 24-channel, fixed-gain, 16-bit recorder. The survey was shot "end-off", with a near-offset of 5 m and a group interval of 5 m. Thus, the length of a shot gather was 115 m, with a far offset of 120 m. Data acquisition parameters were identical for both the pre-shot survey of 27 February and the post-shot

survey conducted on 20 April. Low-cut filters were not used, but a 60-Hz notch filter was used.

Mainly because of poor propagation in the volcanic tuffs, data quality from these surveys varied from fair to poor. The 0.50-caliber rifle, which has been used in some areas to acquire seismic data having frequencies as high as 600 Hz, did not couple well into the surface; the recorded data have most of their energy in the 35-100 Hz band, with a prominent notch from 53-67 Hz due to the use of the 60-Hz notch filter during the recording. The poor source coupling is surely related in part to the dry surface medium. In addition, a prominent, low-velocity (about 300 m/s) wave train contaminates the recorded data. Although this velocity is close to the velocity of air, the wave train is of relatively low frequency, and probably is simply ground roll. Whatever its source, its large amplitude detracts from the ability to resolve reflected energy in portions of the shot gathers. During processing, this wave train was simply muted out of the shot gathers, a procedure that of course eliminates any hope of detecting reflectors in the mute swath.

The 24-channel survey would normally be processed into a 12-fold CDP stack. Miller and Steeples (1992) chose to present a "pseudo 24-fold" CDP section by averaging the CDP traces from adjacent CDP locations. This procedure tends to present a more coherent CDP section, provided that lateral changes are small and that the CDP points are spatially close (in this case the spacing of adjacent CDP gathers is 2.5 m).

The pseudo 24-fold CDP stacked seismic P-wave sections for the pre- and post-shot surveys are shown in Figure 7. There are substantial differences between the two surveys. On the pre-shot survey, a reflector is observed at 250 ms (or about 150 m depth; labeled as reflector "1") and a stacking velocity of 1300 m/s was used. On the post-shot survey two reflectors are now observed and a stacking velocity of 1150 m/s was used representing a 12% reduction in compressional velocity. With this stacking velocity, reflector "1" is now located at 290 ms (still at about 150 m depth) and a new reflector "2" is observed at 210 ms (or about 100 m depth). These stacking velocities correspond well with available uphole travel times collected in U19ba and nearby U19ax (KEARSARGE emplacement hole; location shown on Figure 4). By comparison with the geophysical logs shown in Figure 6, we would expect to observe the strongest reflectors at depths between about 60 to 90 m where the density and velocity contrasts are greatest. At depths close to 150 m, the geophysical characteristics appear to be very uniform and we would not expect to see a strong reflector.

It was also noted that the frequency content for the post-BEXAR survey was slightly higher than that for the pre-shot survey. If the near-surface rocks were damaged as a result of the BEXAR ground motions, we would expect to observe lower frequencies (lower Q) for the post-shot survey. The NTS experienced heavy rains during the month of March and it is possible that near-surface ground saturation may have been more favorable to the transmission of higher frequencies for the post-shot survey.

The actual causes for the differences between the pre- and post-shot surveys are unclear at this time. The simplest explanation is that the near-surface rocks were damaged as a result of the passage of the high-amplitude stress wave causing a reduction in the material velocity and that a spall detachment surface generated the new reflector observed at about 100 m depth on the post-shot survey. However, a number of observations (discussed below) argue against this and the cause for the differences between the pre- and post-shot survey remains uncertain.

LANL fielded 48 portable accelerometer stations as part of an Integrated Verification Experiment (IVE). One station (station 24; Figure 4) in particular was located in close proximity to line 2 near the expected edge of spall. The acceleration and velocity records from station 24 are shown in Figure 8. From the acceleration records, it appears spall did not occur at line 2, although the edge of spall must have been very close. Peak vertical accelerations on the second major upswing (which would be the slap down phase on a spall record) are 8.0 m/s^2 ($1 \text{ g} = 9.8 \text{ m/s}^2$). Thus, it is difficult to believe that the second reflector in the line 2 post-shot survey is from a spall detachment surface.

From the velocity records, we can estimate the vertical strains from the ratio of the particle velocity to the phase velocity. The maximum particle velocity at station 24 is 0.5 m/s. Assuming a surface velocity of 1000 m/s we estimate the vertical strain, e_{zz} , to be approximately 5×10^{-4} . Next, we can estimate the pressures, P , involved at the near surface from the relationship $P = (3\lambda + 2\mu) e_{zz}$. Assuming $V_p = 1000 \text{ m/s}$, $V_s = 577 \text{ m/s}$, $\rho = 2 \text{ Mg/m}^3$, and $e_{zz} = 10^{-3}$, we obtain an estimate of the near-surface pressure to be 3.3 MPa (or 33 bar). We have plotted these values on stress-strain plots for the Ammonia Tanks Tuff and Rainier Mesa Tuff from Pahute Mesa (Figure 9; Gardiner and Butters, 1978). From the location of the points on Figure 9 it is difficult to believe that the stresses were sufficient to damage the tuffs enough to cause a 12% velocity reduction. It appears that the tuff would have behaved linearly under these stress conditions. On the other hand, the physical properties of tuff can be highly variable and if the near-surface rocks were damaged and weakened as a result of the nearby KEARSARGE and LABQUARK

explosions, then it may be possible that the near-surface rocks could have been further damaged by BEXAR. Also, lab measurements may not be representative of the bulk physical properties of the in situ rock.

The other possibility for the reflection observations is that the near-surface material properties changed in the region as the result of a substantial amount of precipitation occurring in the month of March (in the time period between the two surveys). As noted above, the frequency content changed in the pre- and post-shot surveys (higher frequency in the post-shot) possibly due to changes in ground coupling from the source due to ground saturation from the March precipitation. It is possible that the physical properties of the tuffs were changed as a result of increased saturation. It is known that many of the tuff units on Pahute Mesa are characterized by the presence of vertical cooling fractures (in particular the strongly welded tuffs and rhyolites; Warren 1991, unpublished manuscript). From borehole videos, it is known that the welded tuffs of the Ammonia Tanks Tuff are highly fractured in the vicinity of line 2 in the upper 150 m (Figure 6). We expect that the presence of these fractures would increase the bulk permeability of the near-surface rocks thus making them susceptible to changes in saturation state due to surface precipitation.

Numerous papers have been written discussing the effects of saturation on seismic velocities in porous media (e.g. Toksoz *et al.*, 1976; Clark *et al.*, 1980; Gregory, 1976). Porous rocks such as sandstones can show up to a 30% compressional velocity decrease with increased partial saturation (Clark *et al.*, 1980). It is thought that this can be due to a combination of factors including fluid flow between adjacent microcracks (Mavko and Nur, 1979), weakening of the cementing clay minerals in the rock matrix (Clark *et al.*, 1980), and changes in the surface energy (affecting the cohesive forces) by the adsorbed fluid (Murphy *et al.*, 1984). The effect of partial saturation on the elastic modulus is due to many complicated factors such as lithology, texture, pore geometry, fluid chemistry and viscosity. Whatever the mechanism, it is possible that the velocity reduction is due to the effect of different saturation conditions in the upper few hundred meters between the pre- and post-shot surveys. This is illustrated in Figure 10 (modified from Gregory, 1976) which is a schematic showing variations in P-wave velocity as a function of water saturation for sedimentary rocks. The curve is representative for a high porosity (> 25%) rock at moderate confining pressure (~ 35 MPa). It should be noted that air saturation is the ratio of gas-filled porosity to total porosity in this figure. We have highlighted the range expected for the near-surface tuffs. It is possible that the saturation state of the tuffs

changed as a result of the extensive March rains, thereby reducing the in situ compressional velocity.

The appearance of the second reflector at 100 m depth remains problematical. The geophysical measurements shown in Figure 6 indicate that the porosity and gas-filled porosity values are very high just above 100 m depth. Thus, this unit could have been more strongly affected by the hypothesized change in saturation. Alternatively, the caliper logs shown in Figure 6 show a zone of hole enlargement between depths of 107 to 123 m which could indicate a weak layer. It is possible (though not likely) that this layer was deformed as a result of the passage of the signals from BEXAR. However, caliper logs from U19ax (KEARSARGE; Figure 4) do not show this feature.

RECOMMENDATIONS FOR FUTURE WORK

Although the results of this study are inconclusive, we are encouraged that small differences between pre- and post-shot reflection surveys can be mapped in the vicinity of nuclear explosions. If the technique is successful, it holds promise for inexpensively delineating the lateral and depth extent of spall from nuclear explosions. Many of the difficulties encountered in this experiment were due to uncertainties in performing reflection surveys in volcanic tuffs. More energetic sources (small high-explosive charges) would improve the wave propagation through the highly attenuation tuff units, but the experiment would become prohibitively expensive. In the next experiment, a 48 channel system will be used and another attempt will be made to collect shear-wave data using a system with the proper recording bandwidth and a longer profile. The ground motion recordings were critical in understanding what happened in the vicinity of the reflection lines. In the future experiment we will attempt to not only obtain ground-motion data adjacent to the reflection line, but also downhole data from any nearby boreholes that may exist.

ACKNOWLEDGMENTS

We wish to thank Michael C. Fehler for useful discussions regarding wave propagation in partially saturated rocks and Fred App for effects of strong ground motions on material properties. We also thank Fred App and Carl Newton for review of the manuscript. This work is performed under the auspices of the U.S. Department of Energy by Los Alamos National Laboratory under contract W-7405-ENG-36.

REFERENCES

- App, F.N. and W.M. Brunish, Stress wave calculations of four selected underground nuclear tests: Merlin, Hearts, Presidio, Misty Echo, *Los Alamos National Laboratory*, Report EES-NTC-91-03, 65pp, 1991.
- App, F.N. and W.M. Brunish, Modelling surface motion and spall at the Nevada Test Site, *Los Alamos National Laboratory, Los Alamos, NM*, LAUR-92-500, 60pp, 1992.
- Bakun, W.H. and L.R. Johnson, The deconvolution of teleseismic P waves from explosions MILROW and CANNIKIN, *Geophys. J. R. astr. Soc.*, 34, 321-342, 1973.
- Burdick, L.J., T. Lay, D.V. Helmberger, and D.G. Harkrider, Implications of records from the spall zone of the Amchitka tests to nonlinear losses in the source region and to elastic radiation by spall, Woodward Clyde Consultants, WCCP-R-84-03, Pasadena, CA, 37pp, 1984.
- Burdick, L.J., C.K. Saikia, and D.V. Helmberger, Deterministic modeling of regional waveforms from the Nevada Test Site, Air Force Geophysics Laboratory, GL-TR-89-0196, Hanscom Air Force Base, MA, 69pp, 1989.
- Clark, V.A., B.R. Tittmann, and T.W. Spencer, Effect of volatiles on attenuation (Q^{-1}) and velocity in sedimentary rocks, *J. Geophys. Res.*, 85, 5190-5198, 1980.
- Day, S.M. and K.L. McLaughlin, Seismic source representations for spall, *Bull. Seism. Soc. Am.*, 81, 191-201, 1991.
- Day, S.M., N. Rimer, and J.T. Cherry, Surface waves from underground explosions with spall: Analysis of elastic and nonlinear source models, *Bull. Seism. Soc. Am.*, 73, 247-264, 1983.
- Eisler, J.D., F. Chilton, and F.M. Stauer, Multiple subsurface spalling by underground nuclear explosions, *J. Geophys. Res.*, 71, 3923 - 3927, 1966.
- Gardiner, D.S. and S.W. Butters, Material characterization of UE19X drill hole tuffs, *Terra Tek Report, Salt Lake City, Utah*, TR 78-37, 22pp, 1978.
- Gregory, A.R., Fluid saturation effects on dynamic elastic properties of sedimentary rocks, *Geophys.*, 41, 895 - 921, 1976.
- Hansen, R.A., F. Ringdal, and P.G. Richards, The stability of RMS Lg measurements and their potential for accurate estimation of the yields of Soviet underground nuclear explosions, *Bull. Seism. Soc. Am.*, 80, 2106-2126, 1990.
- Kennett, B.L., *Seismic Wave Propagation in Stratified Media*, Cambridge University Press, Cambridge, 342pp, 1983.
- Mavko, G.M., and A. Nur, Wave attenuation in partially saturated rocks, *Geophysics*, 44, 161-178, 1979.

- McLaughlin, K.L., T.G. Barker, S.M. Day, B. Shkoller, and J.L. Stevens, Effects of depth of burial and tectonic strain release on regional and teleseismic explosion waveforms, S-Cubed Scientific Report, SSS-R-88-9844, 116pp, 1988.
- Miller, R. and D. Steeples, Seismic reflection surveys before and after BEXAR at the Nevada Test Site, Los Alamos National Laboratory, Report LAUR-92-244, 20pp, 1992.
- Mueller, R.A., and J.R. Murphy, Seismic characteristics of underground nuclear explosions, Part 1 seismic spectrum scaling, *Bull. Seism. Soc. Am.*, 61, 1675-1692, 1971.
- Murphy, W.F., K.W. Winkler, and R.L. Kleinberg, Frame modulus reduction in sedimentary rocks: The effect of adsorption on grain contacts, *Geophys. Res. Lett.*, 1, 805-808, 1984.
- Patton, H.J., Source models of the Harzer explosion from regional observations of fundamental-mode and higher mode surface waves, *Bull. Seism. Soc. Am.*, 78, 1133-1157, 1988.
- Patton, H.J., Estimates of spall mass and spall impulse from observed strong ground motions on Pahute Mesa, *Bull. Seism. Soc. Am.*, 80, 1326-1345, 1990.
- Patton, H.J., Seismic moment estimation and the scaling of the long-period explosion source spectrum, in *Explosion Source Phenomenology*, AGU Monograph 65, (Taylor, S.R., H.J. Patton, and P.G. Richards, eds.), 171-183, 1991.
- Patton, H.J., and S.R. Taylor, Spall source parameters from the spectral ratios of Lg waves, *Trans. Am. Geophys. Un.*, 43, 1478, 1990.
- Rygg, E., Anomalous surface waves from underground explosions, *Bull. Seism. Soc. Am.*, 69, 1995-2002, 1979.
- Sobel, P.A., The effect of spall on m_b and M_s , Teledyne Geotech Report SDAC-TR-77-12, Dallas, Texas, 1978.
- Stump, B.W., Constraints on explosive sources with spall from near-source waveforms, *Bull. Seism. Soc. Am.*, 75, 361-377, 1985.
- Springer, D.L., Secondary sources of seismic waves from underground nuclear explosions, *Bull. Seism. Soc. Am.*, 64, 581-594, 1974.
- Taylor, S.R., and G.E. Randall, The effects of spall on regional seismograms, *Geophys. Res. Lett.*, 16, 211-214, 1989.
- Toksoz, M.N., C.H. Cheng, and A. Timur, Velocities of seismic waves in porous rocks, *Geophysics*, 41, 621-645, 1976.
- Viecelli, J.A. Spallation and the generation of surface waves by an underground explosion, *J. Geophys. Res.*, 78, 2475 - 2487, 1973.

FIGURE CAPTIONS

Figure 1. Schematic showing the formation of spall above a buried explosion. The compressional wave reflected off the free surface interferes with the tail of the upgoing wave. The material fails in tension and goes into ballistic free flight. The acceleration spall signals are characterized by up upward pulse from the impinging compressional wave, followed by a -1 g dwell, followed by another upward pulse from the subsequent slapdown of the spalled layer. The spalled layer thickness and observed accelerations and dwell times decrease with distance from ground zero.

Figure 2. Effects of spall dwell time (left; T_s) and rise time (right; T_{sr}) on source spectra. The dwell time is related to the escape velocity (v_0) through simple ballistics, $T_s = 2v_0/g$, where g is the gravitational acceleration (9.8 m/s^2). First number in figure labels corresponds to the spall dwell time and the second number to the spall rise time (in seconds). Spall signals computed using the model of Stump (1985).

Figure 3. Comparison of explosion and spall synthetic seismograms. The explosion and spall responses are shown in the top and bottom three panels, respectively. The left panel shows the source-time functions, the middle panel the point-source response, and the right panel the complete explosion and spall response (formed by convolving the source-time function with the point-source response; see text for details).

Figure 4. Map showing location of U19ba (BEXAR emplacement hole), predicted maximum extent of spall (at 1.8 km), location of reflection lines 1 and 2 and acceleration stations discussed in text. Holes U19an and U19ax are LABQUARK and KEARSARGE emplacement holes, respectively.

Figure 5. East-west cross section through U19ba (BEXAR emplacement hole; Warren 1991, unpublished manuscript). Key to symbols: Tm - Timber Mountain Group; Tma - Ammonia Tanks Tuff; Tmr - Rainier Mesa Tuff; Tmrh/Tcps - tuff of Holmes Road/rhyolite of Sled (Crater Flat Group); Tcpg + Tcg - rhyolite of Kearsarge + andesite of Grimy Gulch; Tcb + Tct - Bullfrog Tuff + Tram Tuff; Tb - Belted Range Group.

Figure 6. Geophysical logs for the BEXAR emplacement hole (U19ba).

Figure 7. (a) Pseudo 24-fold CDP stacked seismic section from pre-shot line 2. Stacking velocity of 1300 m/s utilized in stacking. Note coherent reflection (indicated by arrow) "1" at 250 ms (or about 150 m depth). (b) Pseudo 24-fold CDP stacked seismic section from post-shot line 2. Stacking velocity of 1150 m/s utilized in stacking. Note addition of new reflector "2" at 210 ms (at about 100 m depth). Reflector "1" is now at 290 ms (still at about 150 m depth; both reflectors indicated by arrows).

Figure 8. (a) Acceleration and (b) velocity records for station 24 (see Figure 4 for location).

Figure 9. Unconfined compression tests, stress versus axial and transverse strains for Ammonia Tanks Tuff (top) and Rainier Mesa Tuff (bottom) from hole UE19X on Pahute Mesa (Gardiner and Butters, 1978). Different lines correspond to samples from

depths indicated in feet. Circles correspond to estimated free surface strains and pressures recorded at Station 24 for BEXAR (see text for details).

Figure 10. Schematic illustration showing the variation of P-wave velocity as a function of air saturation for a porous ($> 25\%$) sedimentary rock at a confining pressure of about 35 MPa). The range of air saturation for the near-surface tuffs in the vicinity of BEXAR is highlighted (modified from Gregory, 1976). In this figure, air saturation is the ratio of gas-filled porosity to total porosity.

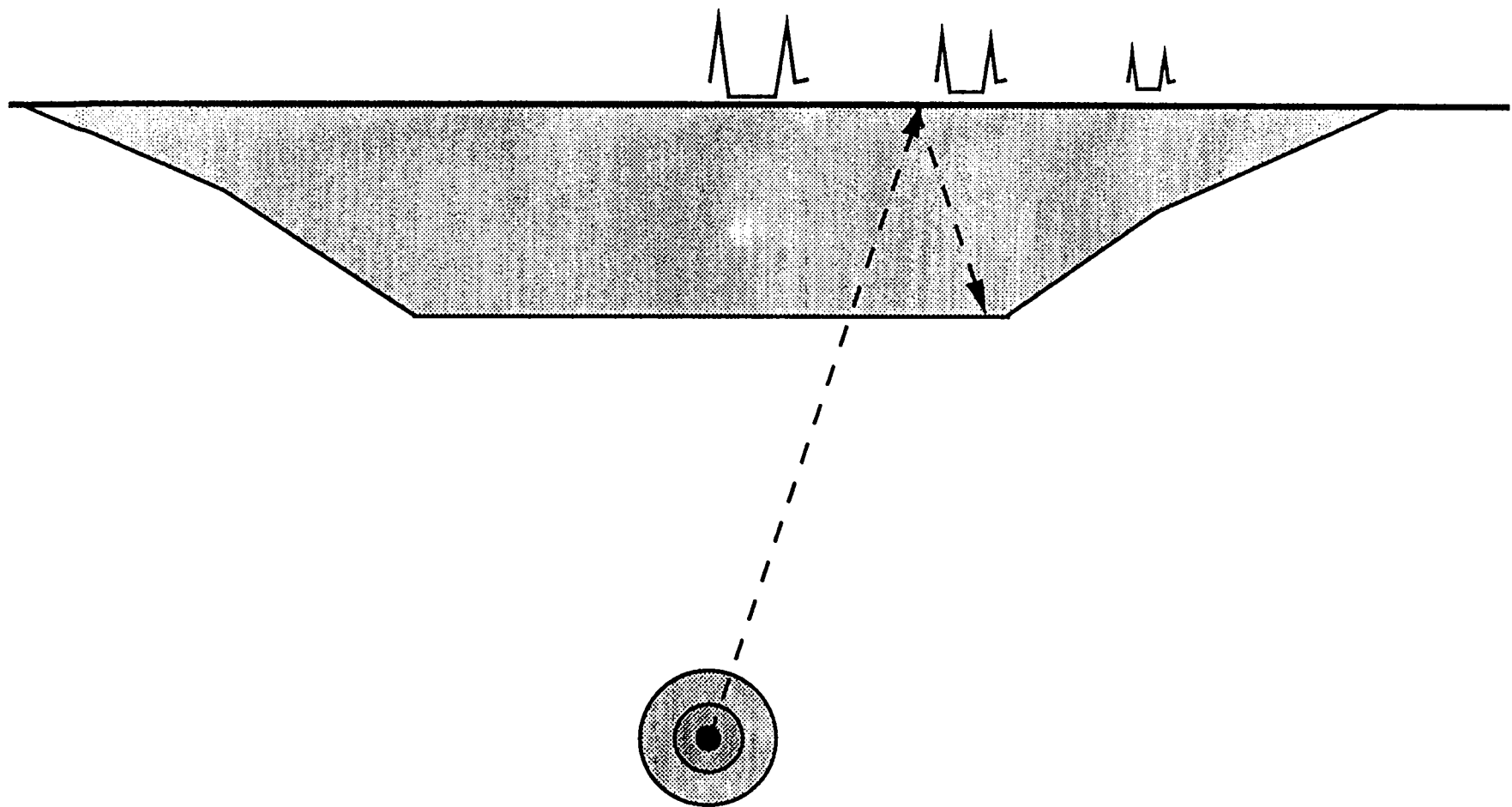


Figure 1

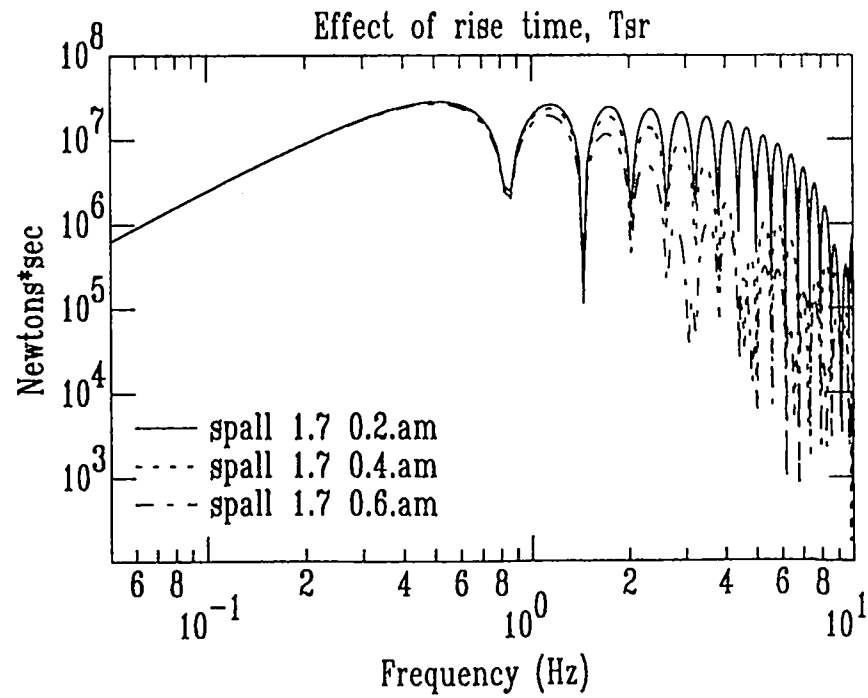
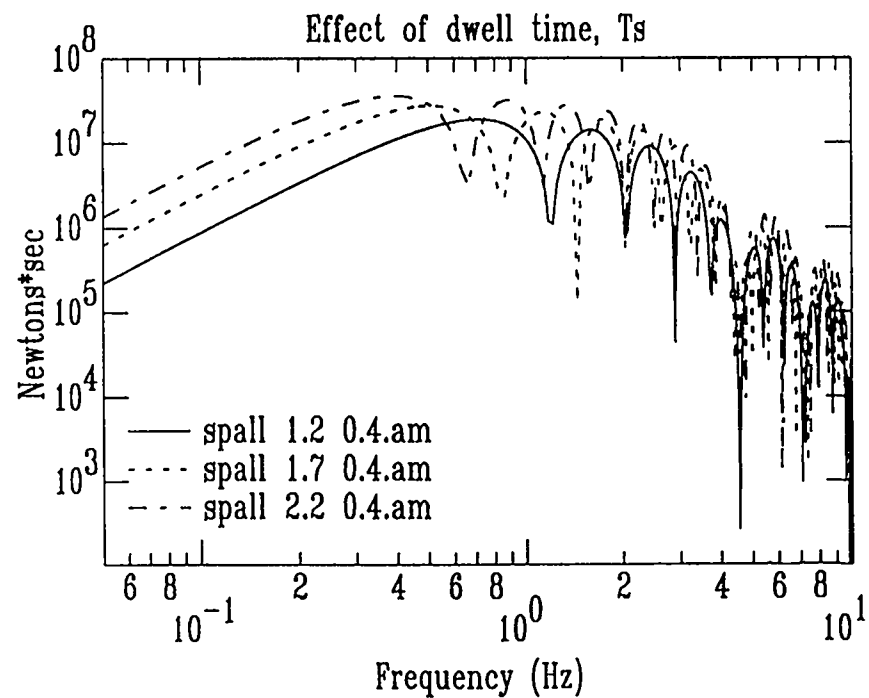
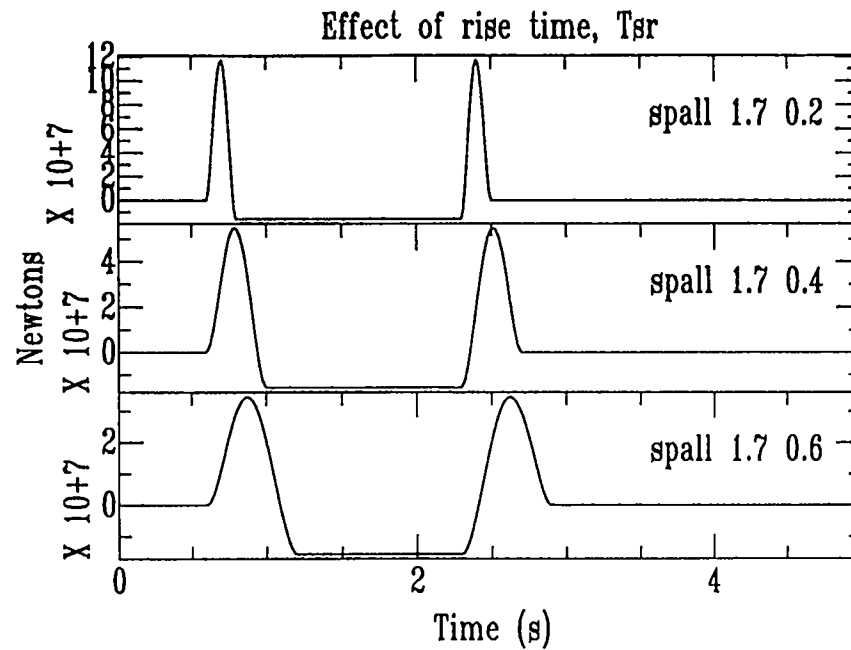
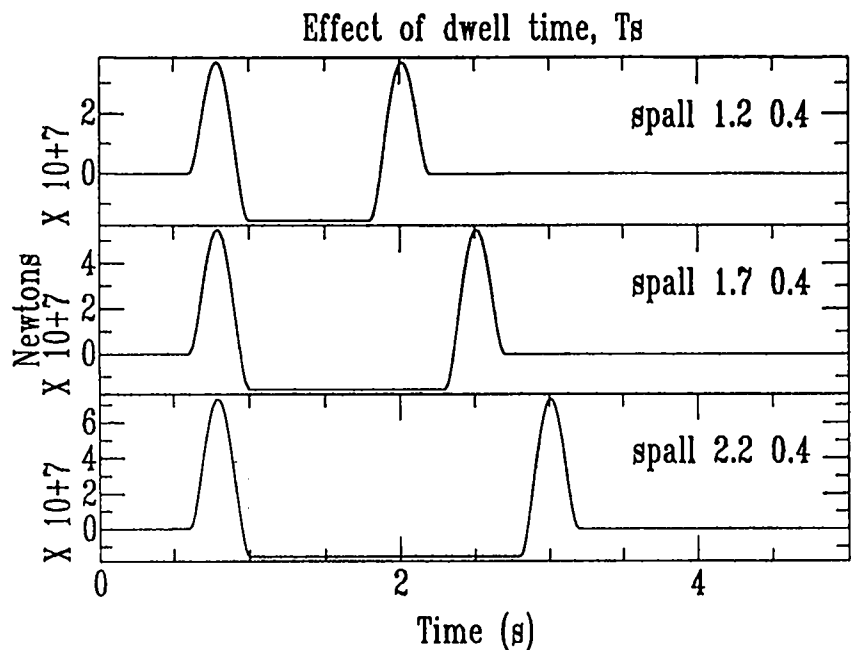


Figure 2

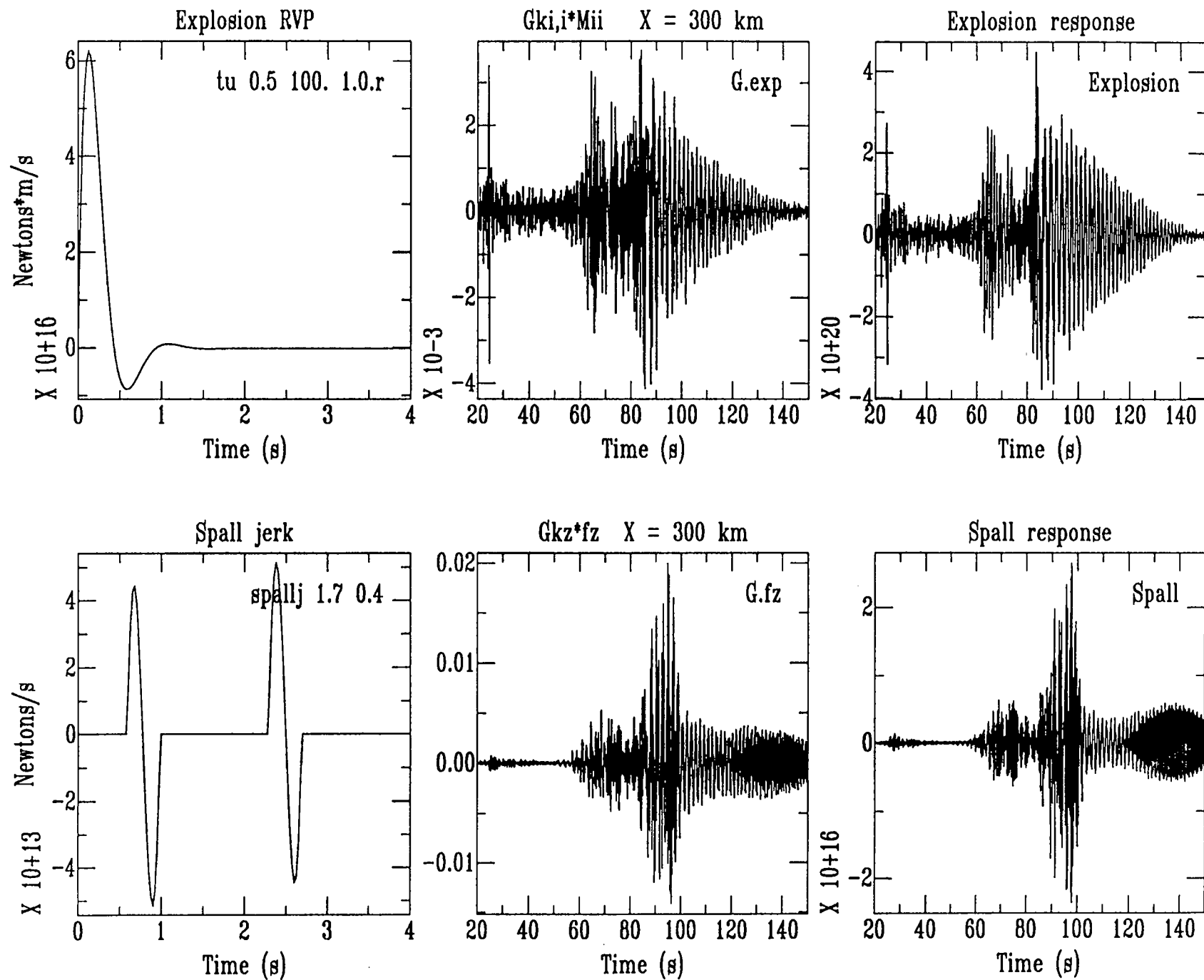


Figure 3

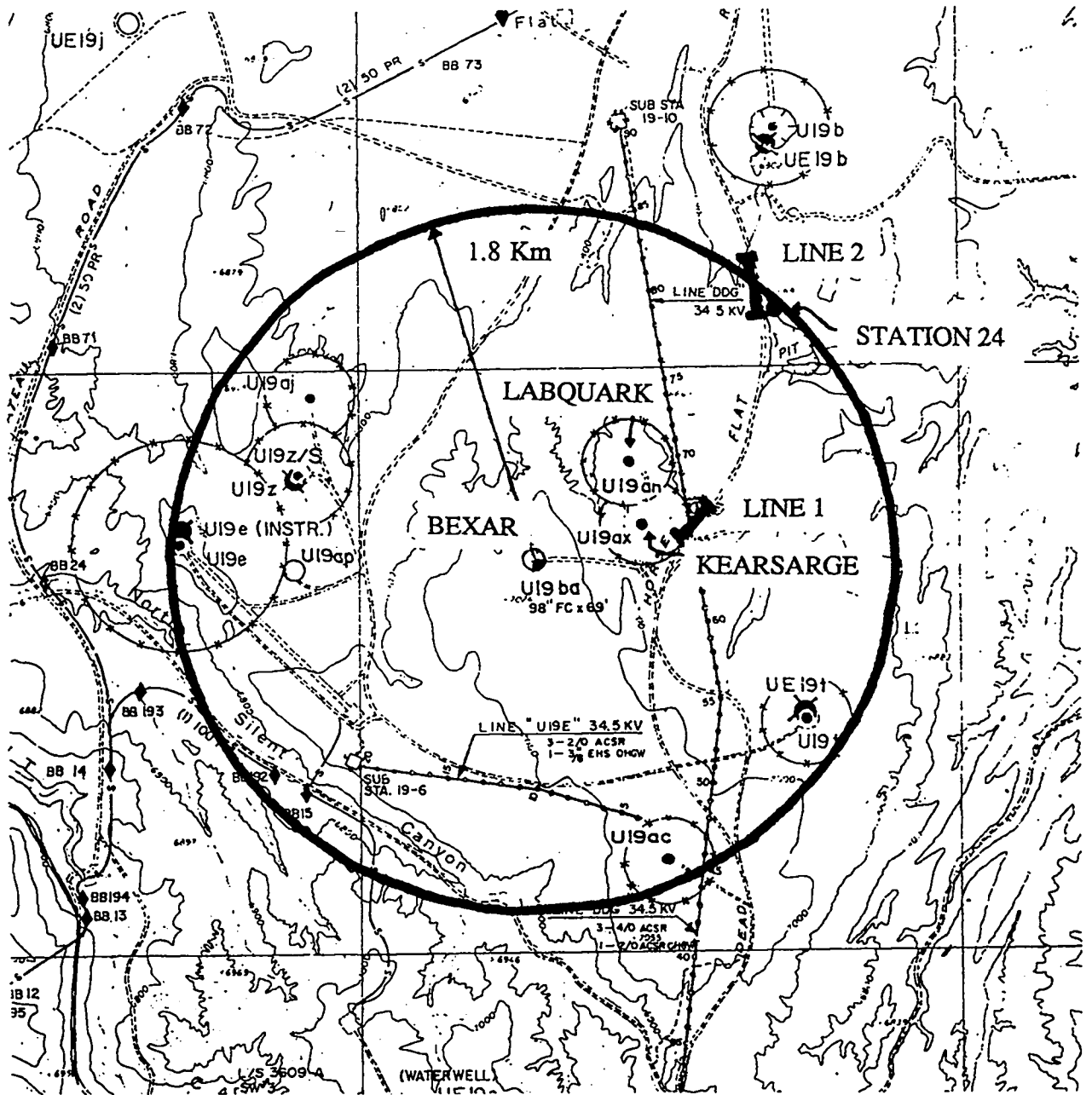


Figure 4

WEST-EAST GEOLOGIC CROSS SECTION FOR U19ba

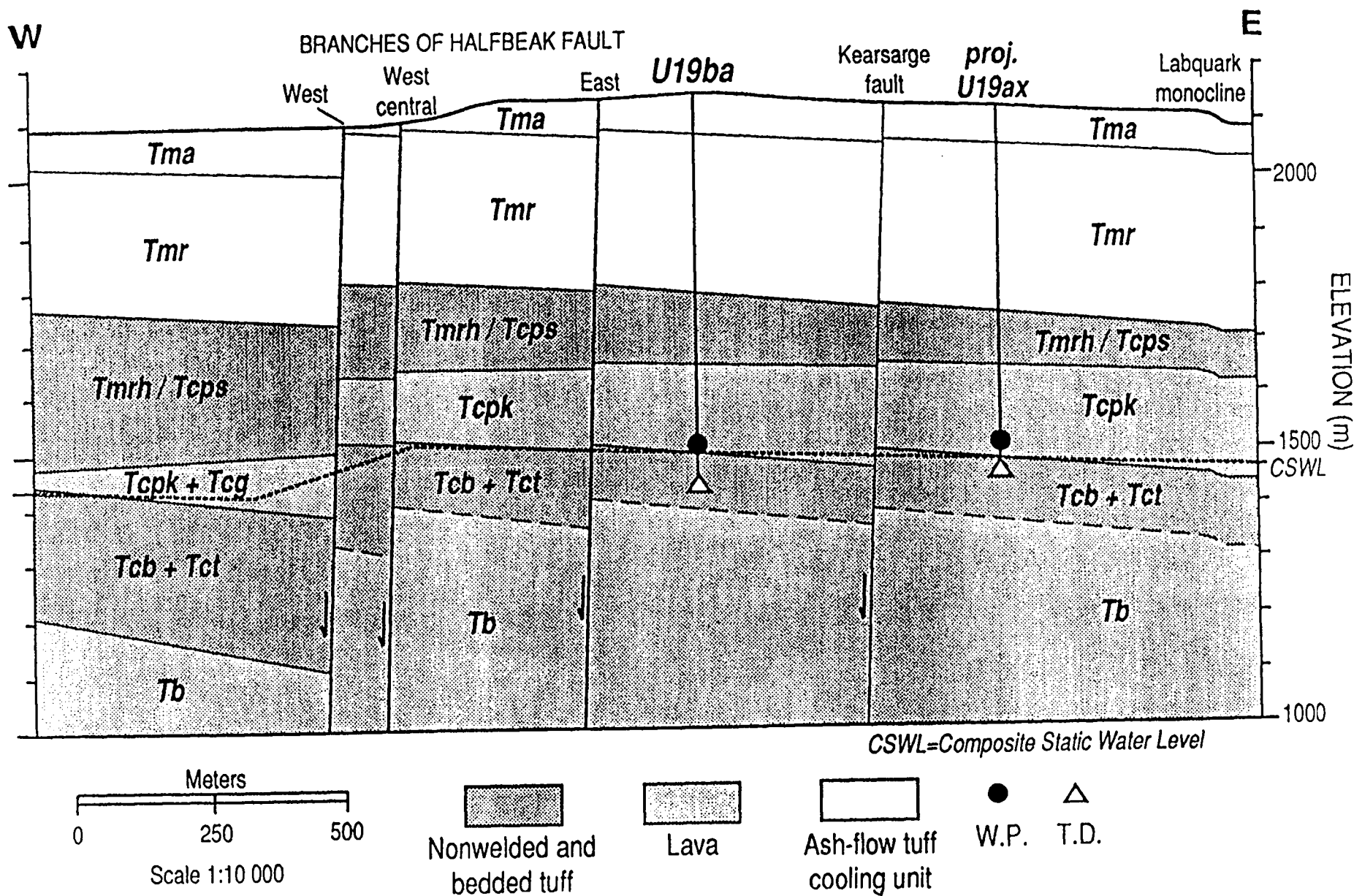


Figure 5

U19BA

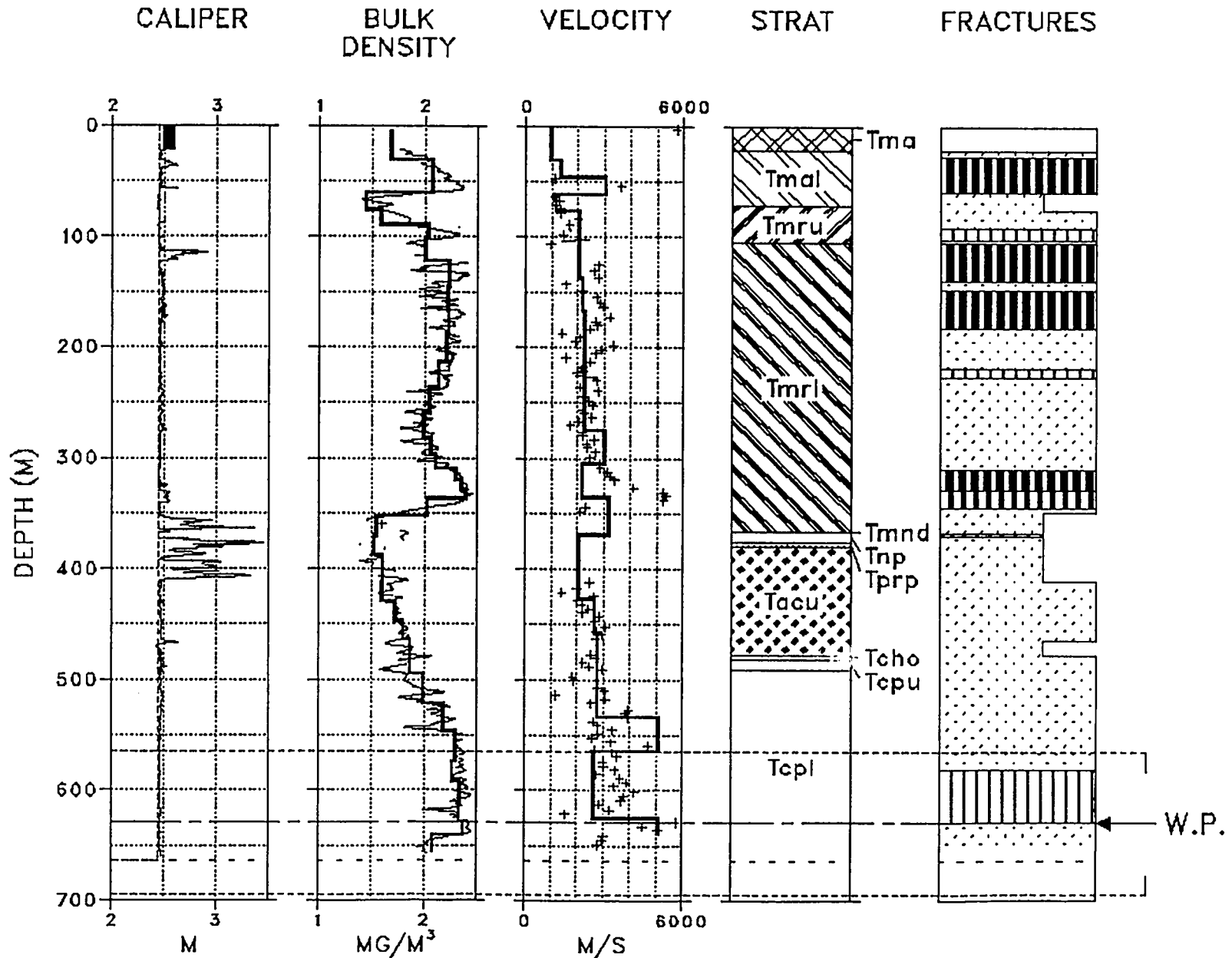
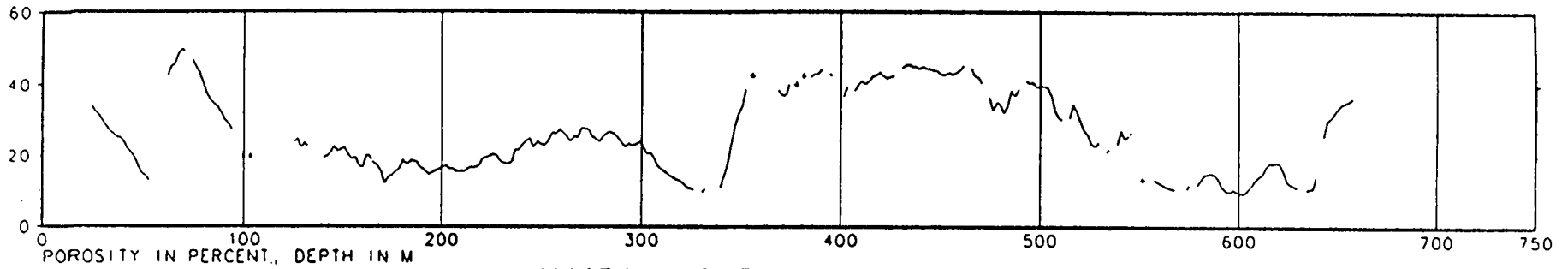


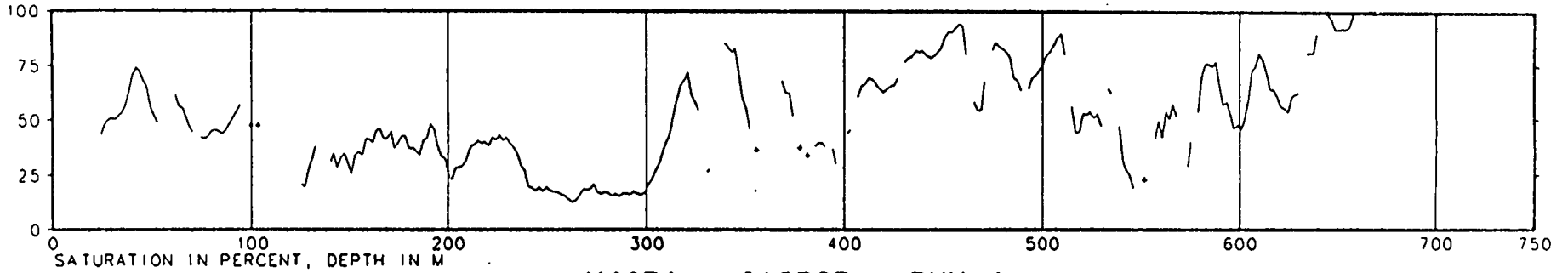
Figure 6

Figure 6 (continued)

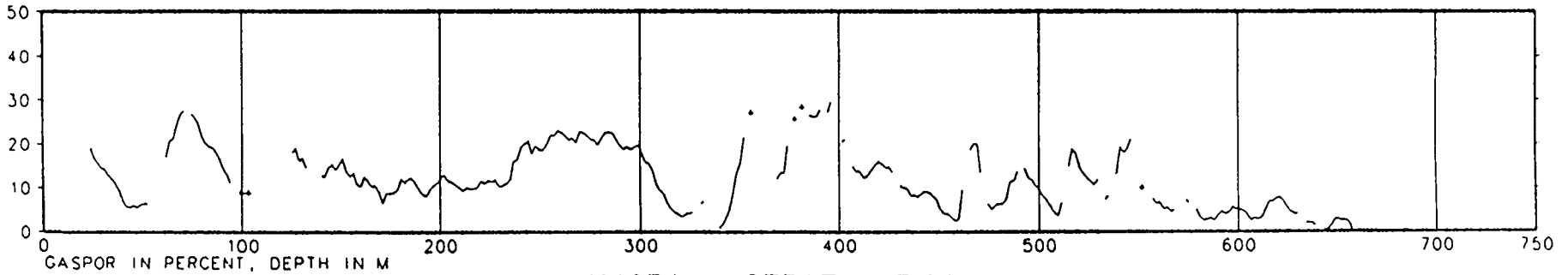
U19BA - POROSITY - RUN 1



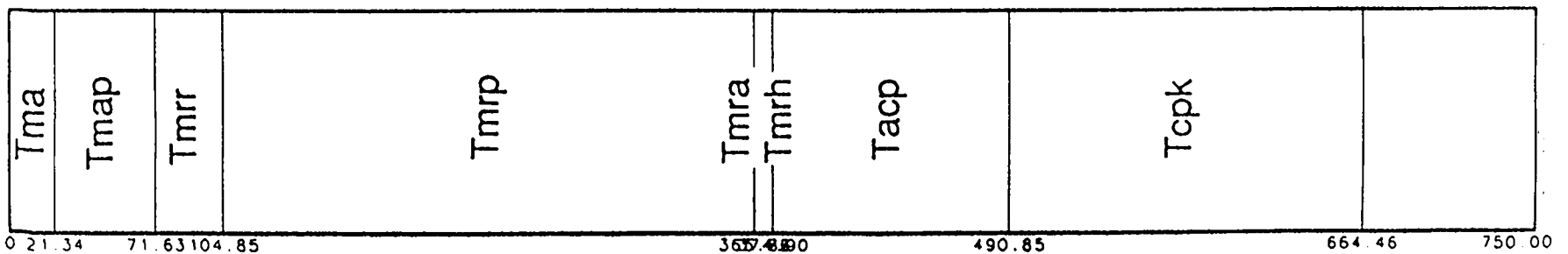
U19BA - SATURATION - RUN 1

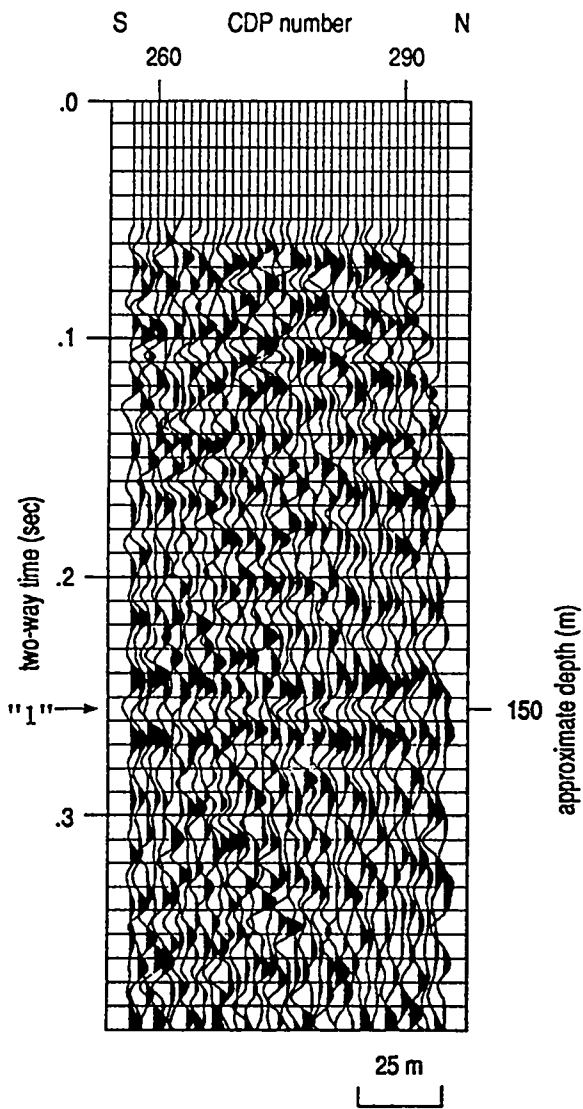


U19BA - GASPOR - RUN 1

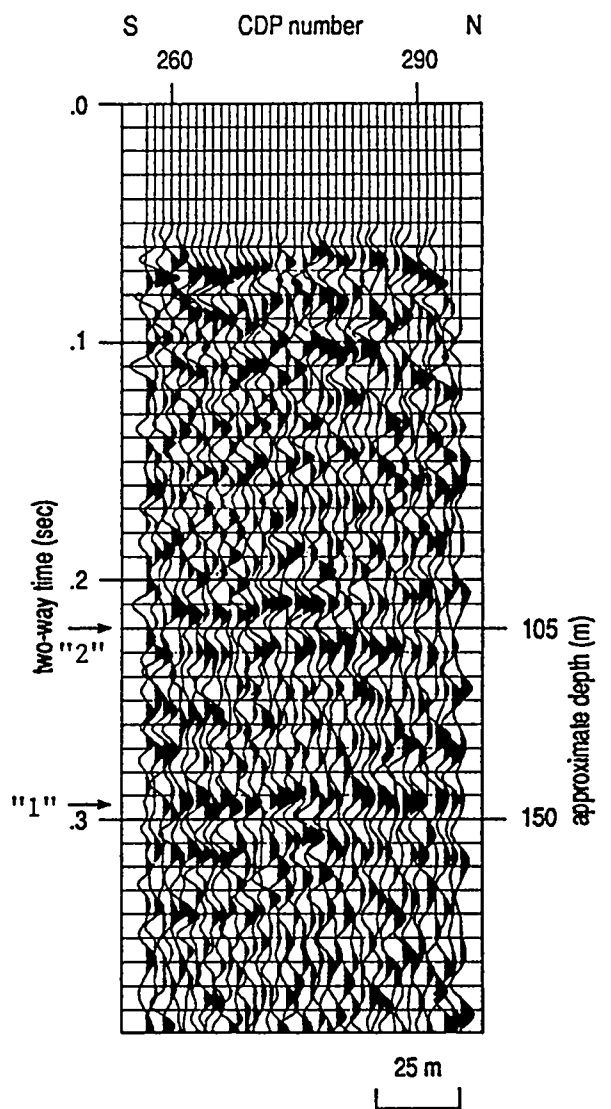


U19BA - STRAT - RUN 1





(a)



(b)

Figure 7

BEXAR Station 24 Acceleration

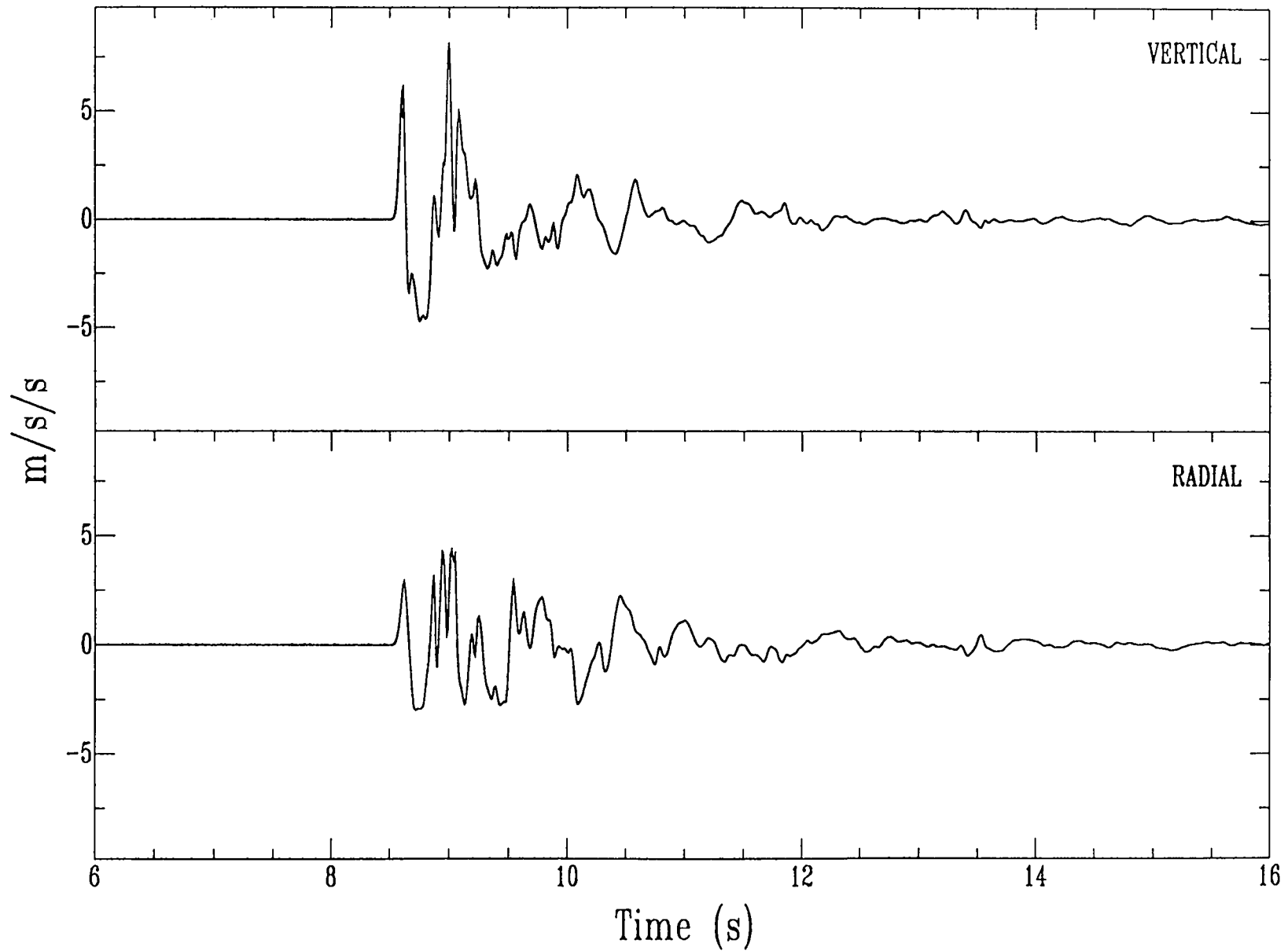


Figure 8a

BEXAR Station 24 Velocity

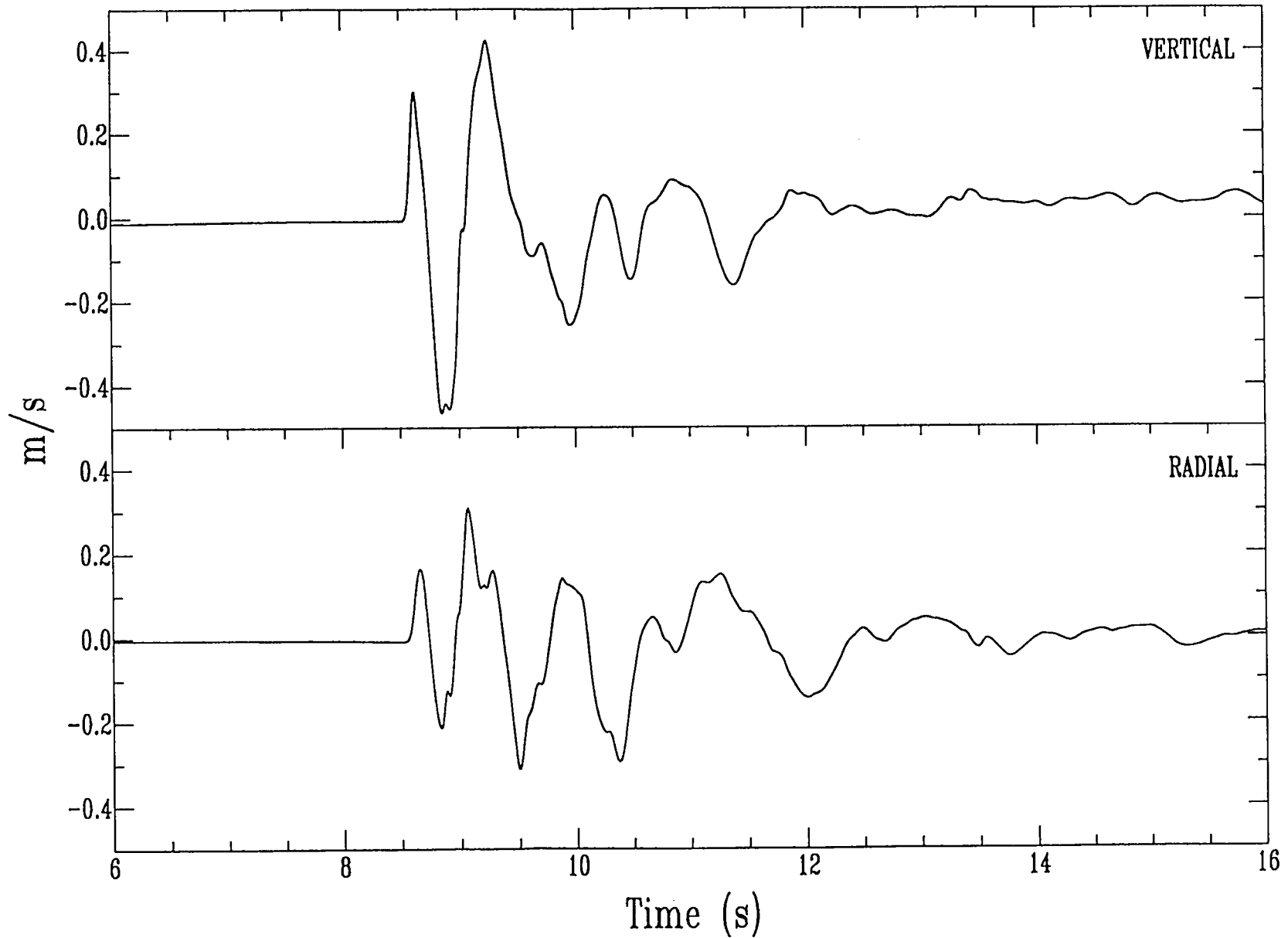


Figure 8b

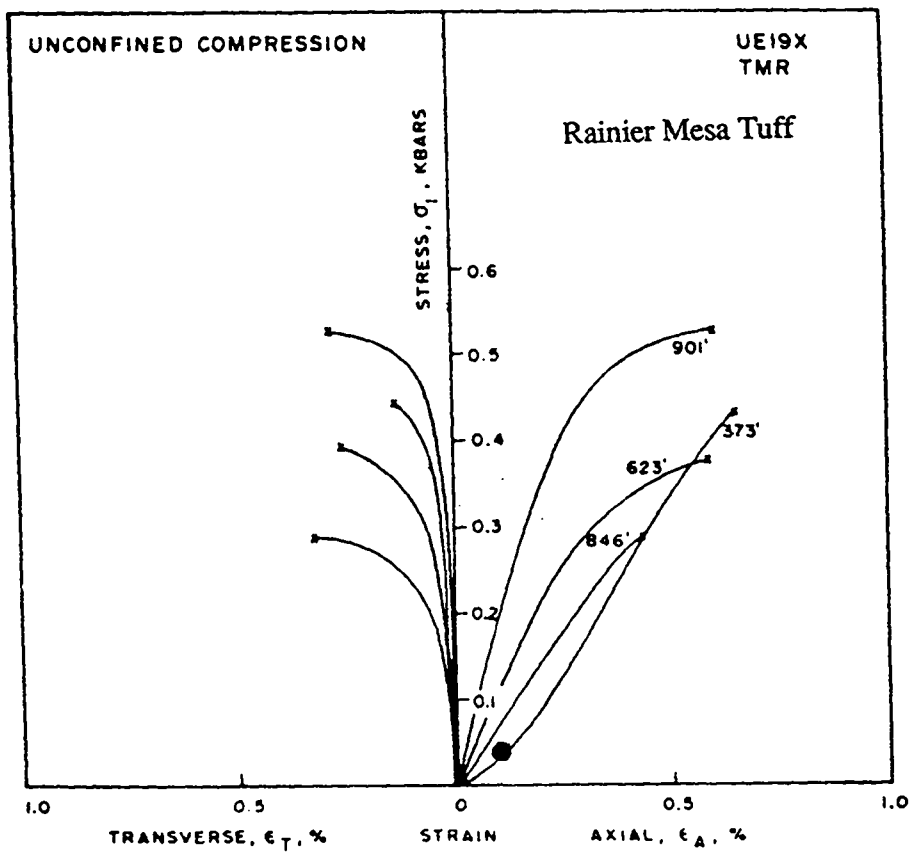
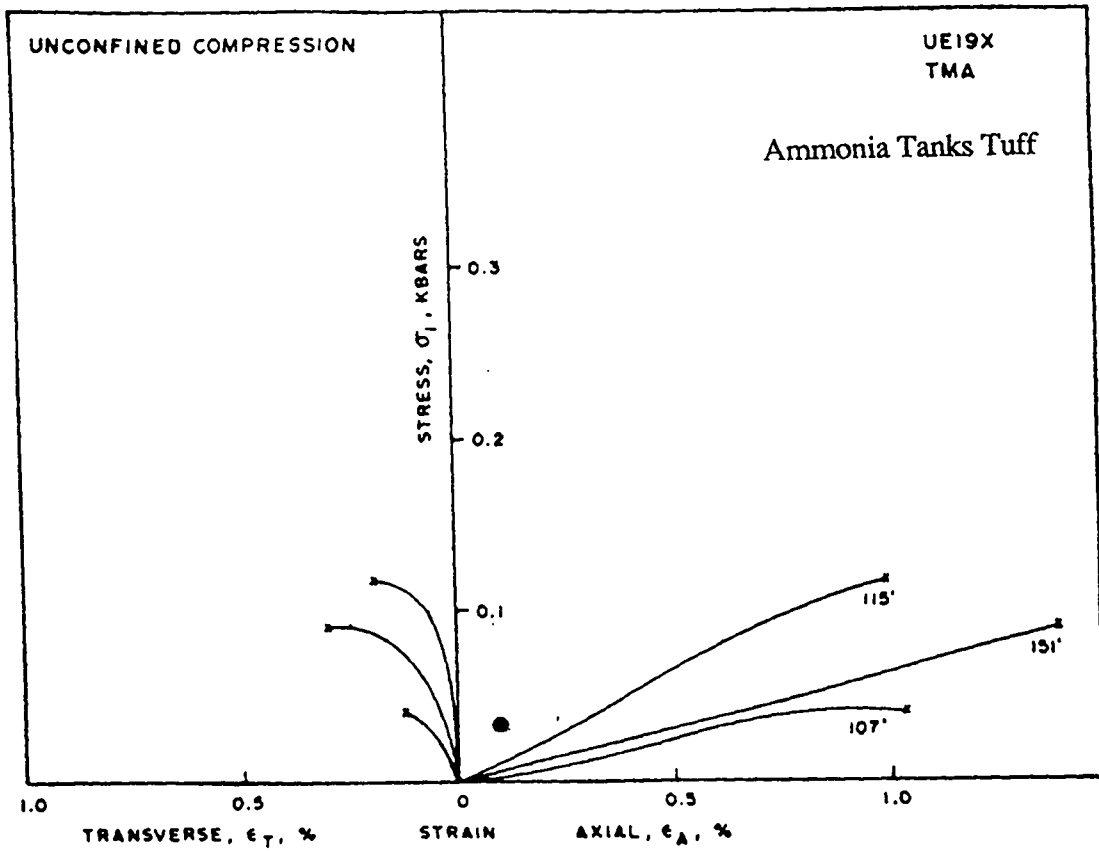


Figure 9

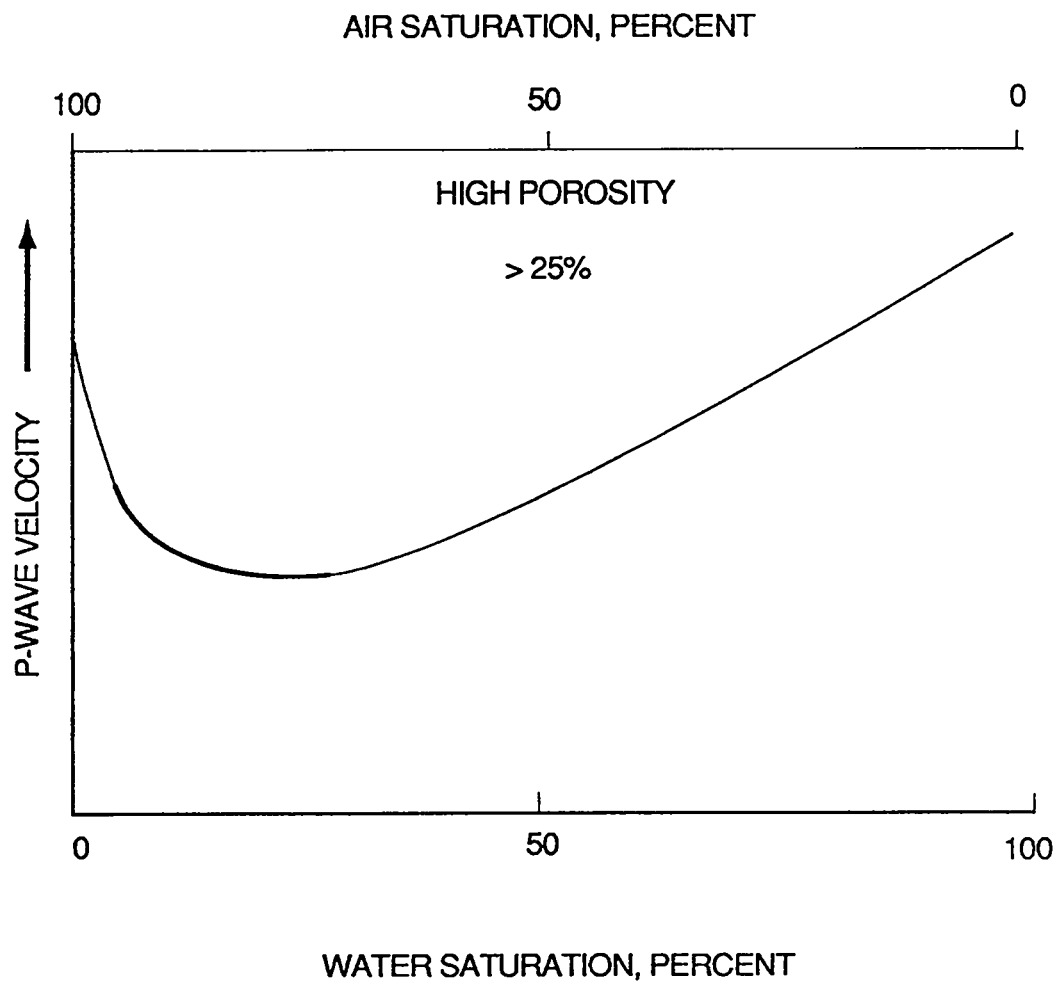


Figure 10